Surface Science 135 (1983) 396–408
North-Holland Publishing Company

PREPARATION AND CHARACTERIZATION OF Cu(111)–Ni AND Cu(110)–Ni SURFACE ALLOYS

C.M.A.M. MESTERS, G. WERMER, O.L.J. GIJZEMAN and J.W. GEUS

Van 't Hoff Laboratory, University of Utrecht, Padualaan 8, 3584 CH Utrecht, The Netherlands

Received 7 February 1983; accepted for publication 18 May 1983

The interaction of $Ni(CO)_4/CO$ gas mixtures with Cu(111) and Cu(110) single crystal surfaces has been studied with ellipsometry, Auger electron spectroscopy, LEED and argon ion depth profiling. At room temperature Ni atoms with some CO ligands remain at the surface. The amount of Ni that can be deposited is less than one monolayer. The alloy surface is able to bind CO. After exposures above 220°C, the initially deposited amount of Ni resides below the first layer of Cu atoms. The amount of Ni that can be deposited is essentially unlimited. The alloy surfaces show no contamination of C or O at the surface or in deeper layers. The Ni concentration profile below the surface is bell shaped and is metastable up to 400–450°C. The ellipsometric data can be understood if one assumes that a significant fraction of voids are present in the Cu–Ni layer.

1. Introduction

The practical importance of alloys in heterogeneous catalysis is widely known. Unsupported alloys, used to study the structure and reactivity in UHV systems with surface analytical equipment, are generally prepared by melting the pure components together in an unreactive crucible. A second method of preparing alloys is vapour deposition of one metal on the surface of another. As has been published before [1], it is also possible to obtain surface alloys by exposing a metal surface to a volatile metal compound (such as $Ni(CO)_4$). It was shown that Cu(100)–Ni surface alloys, with a reproducible amount of Ni in the surface layers, could thus be prepared. In this paper we report on the preparation of Cu(111)–Ni and Cu(110)–Ni alloys by decomposition of $Ni(CO)_4$. The deposition of Ni is continuously monitored with ellipsometry and the surface layers have been characterized with Auger electron spectroscopy, LEED and Ar ion depth profiling. Some results on the chemistry of these surface alloys have been presented previously [2,3].

2. Experimental

The experiments were performed in a standard UHV system [4] provided with facilities for AES, LEED and ellipsometry. Auger spectra were recorded

0039-6028/83/0000–0000/$03.00

with a four-grid retarding field analyser. The current of the primary beam was 30 μA, its energy 2500 eV and the angle of incidence 7° with the plane of the surface. The modulation voltage was 2 $V_{p\text{-}p}$ for the low energy part of the spectrum (95–110 eV). Since the mean effective escape depth λ of electrons with this energy is about 3.6 Å [5], the amount of nickel in this layer can be found from $x_L = k_L h_{101}/(k_L h_{101} + h_{105})$ where h_{101} and h_{105} are the peak-to-peak heights of the Ni ($M_1M_{4,5}M_{4,5}$) 101 eV and Cu ($M_1M_{4,5}M_{4,5}$) 105 eV peaks in the derivative Auger spectra. k_L is the relative elemental sensitivity factor, taken to be 1.4 [5]. The high energy part of the spectrum was recorded with a modulation voltage of 10 $V_{p\text{-}p}$. Since λ is larger for electrons with energies between 720 and 920 eV, the amount of nickel x_H in the first 6–8 atomic layers can be calculated from $x_H = k_H h_{720}/(k_H h_{720} + h_{920})$, where k_H is the relative element sensitivity factor between the Ni ($L_3M_{2,3}M_{2,3}$) 720 eV peak and the Cu ($L_3M_{4,5}M_{4,5}$) 920 eV peak which we determined to be 2.5.

The ellipsometric procedure – two-zone measurements and off-null irradiance measurements – was as described in ref. [6]. The parameters $\delta\Delta$ and $\delta\psi$ are defined as $\bar{\Delta} - \Delta$ and $\bar{\psi} - \psi$ respectively, where $\bar{\Delta}$, $\bar{\psi}$ are the values for the clean copper surfaces. For a substrate with an overlayer both $\delta\Delta$ and $\delta\psi$ are in the simplest approximation proportional to the layer thickness or coverage [7]. The two proportionality constants are different, however, and for quantitative analysis the relationship should be established experimentally. The wavelength of the incident light beam was 632.8 nm and the angle of incidence $70 \pm 1°$. The azimuth Ω, defined as the angle between the plane of incidence of the light beam and the [$\bar{1}$10] direction of the (110) surface, was 35° for the two Cu(110) crystals used in this work. Cycles of sputtering (500–800 eV, 5 $\mu A/cm^2$, angle of incidence 45°, 5×10^{-3} Pa Ar) and annealing (450°C) were applied to clean the surfaces. Auger spectra showed that the amount of any contaminant on the surface was less than 0.05 monolayer. Nickel carbonyl was synthesized as described before [1]. Because the fraction of CO in the nickel carbonyl–carbon monoxide gas mixture is unknown, the amount of nickel carbonyl admitted to the vacuum chamber is expressed as total pressure times time. During all exposures the gas was continuously renewed by pumping with the turbomolecular pump.

3. Results

Gas mixtures of $Ni(CO)_4$ and CO were admitted to clean and annealed Cu(111) or Cu(110) surfaces at pressures from 5×10^{-5} to 1 Pa and crystal temperatures of 22 and 220–450°C. Fig. 1 shows the changes in Δ and ψ as a function of time when Cu(110) and Cu(111) were exposed to $Ni(CO)_4$/CO at room temperature. When no further change in $\delta\Delta$ or $\delta\psi$ could be detected, evacuation of the system caused a decrease in $\delta\Delta$ while $\delta\psi$ remained constant.

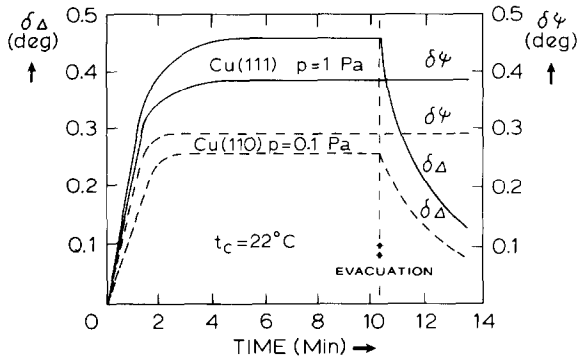

Fig. 1. $\delta\Delta$ and $\delta\psi$ as a function of $Ni(CO)_4/CO$ exposure at room temperature: (— — —) Cu(110), (———) Cu(111).

Auger spectra recorded immediately after evacuation, but before $\delta\Delta$ reached zero, showed besides nickel ($x_H = 0.15$, $x_L = 0.15$ for Cu(110) and $x_H = 0.22$, $x_L = 0.26$ for Cu(111)) also a large amount of carbon, $\theta_C \approx 0.5$ monolayer, and some oxygen. Heating the crystal in vacuum to 270°C decreased the carbon coverage while the oxygen Auger signal disappeared almost completely ($\theta_O <$ 0.05 monolayer). No carbon could be detected when the crystal was first heated to 270°C after a $Ni(CO)_4/CO$ exposure at room temperature.

In fig. 2 the changes in Δ and ψ are depicted as a function of the total exposure ($= p_{total} \times$ time) at constant total pressure and at a crystal temperature of 220°C for Cu(110) and Cu(111). Initially $\delta\Delta$ is negative but it becomes

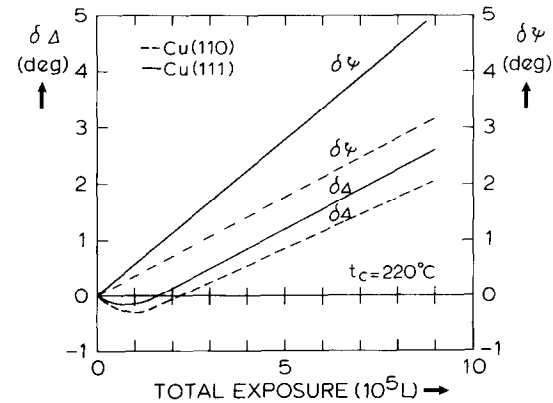

Fig. 2. $\delta\Delta$ and $\delta\psi$ versus $Ni(CO)_4/CO$ exposure at a crystal temperature of 220°C: (— — —) Cu(110), (———) Cu(111).

positive at longer exposures. It appears that the changes in $\delta\Delta$ and $\delta\psi$ are similar on the two crystallographic orientations of the copper surfaces, although the value of $\delta\psi$ at which $\delta\Delta$ becomes positive is significantly smaller for Cu(111) than for Cu(110) (0.5° and 1.2° respectively). Since $\delta\psi$ is linear in the $Ni(CO)_4/CO$ exposure, we assume that in this case $\delta\psi$ is also proportional to the amount of nickel deposited. The reaction rate, defined as $d(\delta\psi)/dt$, appeared to be proportional to p^{α} where α lies between 1 and 2 for both copper surfaces. Due to the way of preparation of $Ni(CO)_4$ and the continuous decomposition of $Ni(CO)_4$ in the UHV system, the partial pressure of $Ni(CO)_4$ is unknown and different for each experiment. For these reasons it is not possible to compare the absolute reaction rates for the two different copper surfaces. After evacuation of the vacuum chamber we observed no change in $\delta\Delta$ and $\delta\psi$ for the Cu(110) surface. The deposition of Ni on Cu(111), however, did not stop immediately. For about 1 min after evacuation $\delta\psi$ increased even more rapidly than during exposure to the $Ni(CO)_4/CO$ mixture. The extent of the change in $\delta\psi$ after evacuation increased with increasing pressure during deposition (0.05° at $p_{total} = 1 \times 10^{-2}$ Pa and 0.2° at $p_{total} = 1$ Pa). This observation is not due to a large background pressure since the time needed to evacuate the system to below 10^{-6} Pa was smaller than the time needed to reach a constant value of $\delta\psi$. No increase in $\delta\psi$ was observed after re-admitting a pressure of 10^{-6} Pa to the vacuum chamber. With Cu(111) we also observed a decrease in $\delta\Delta$ continuing for some minutes after evacuation. Fig. 3 shows an example of the changes in x_L and x_H after increasing $Ni(CO)_4/CO$ exposures at a crystal temperature of 220°C for Cu(111) and Cu(110). Initially there is no evidence for the Ni 101 eV peak although the Cu 105 eV peak slightly decreases. The ratio h_{850}/h_{920}, on the other hand, changes immediately due to an increase in the combined Cu – Ni 850 eV peak and a decrease in the Cu 920 eV peak. Deposition of Ni on Cu(111) and Cu(110) up to $x_H = x_L = 1$ did not cause any detectable contamination of carbon or

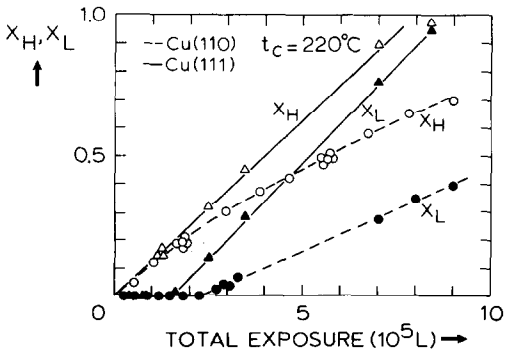

Fig. 3. The average mol fraction of Ni in the first 2 layers (x_L) and first 6–8 layers (x_H) as a function of $Ni(CO)_4/CO$ exposure at 220°C: (— — —) Cu(110), (———) Cu(111).

oxygen. After a $Ni(CO)_4/CO$ exposure, LEED patterns showed no change from the (1×1) structure of pure Cu(111) and Cu(110), although a steady increase in background intensity was observed.

The composition of the surface layers of the Cu(111)–Ni and Cu(110)–Ni alloys, prepared by decomposition of $Ni(CO)_4$, is not constant after evacuation. The nickel content decreases as a function of time at a crystal temperature of 220°C and a background pressure below 10^{-8} Pa. In fig. 4, x_L and x_H are given as a function of time for different amounts of Ni deposited on Cu(111) and Cu(110). x_L is zero for a small amount of nickel deposited and x_H remains constant in this case, as shown by the two horizontal lines in fig. 4 for Cu(111) and Cu(110). When larger amounts of nickel are deposited, both x_H and x_L slowly decrease to a constant value over a period of 100–200 h for both surfaces. When no significant change was observed in x_H and x_L, the alloys were sputtered at room temperature. In fig. 5 the values of x_H and x_L are given as a function of the sputtering time for alloys containing different amounts of nickel. Initially we observe a large increase in x_L and x_H after which the values steadily decrease to zero for both Cu(111)–Ni and Cu(110)–Ni. During these sputter experiments we did not observe any carbon or oxygen.

The amount of nickel in the surface layers was also a function of the crystal temperature. After preparation of the alloy surfaces at 220°C and stabilization at the same temperature, the crystal temperature was changed and the surface composition was measured as a function of time. Decreasing the crystal temperature caused no change in x_H or x_L within the period of two weeks as measured on Cu(110)–Ni. On Cu(111)–Ni, however, we observed a small, though significant, increase in x_H. Increasing the crystal temperature caused a rapid decrease in the values of x_H and x_L after which they remained constant for at least 48 h. These constant values are given in fig. 6 as a function of

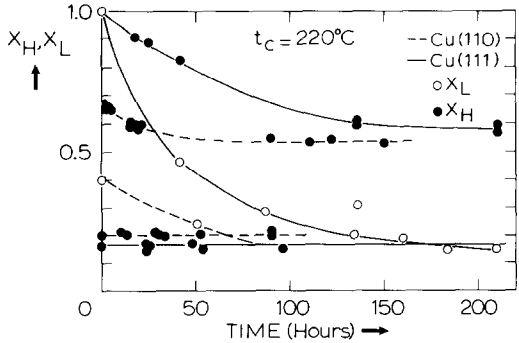

Fig. 4. Changes in x_L and x_H as a function of time at 220°C after Ni deposition on Cu(110) (— — —) and Cu(111) (———) at 220°C. The lower two horizontal lines refer to a small amount of nickel deposited such that $x_L = 0$.

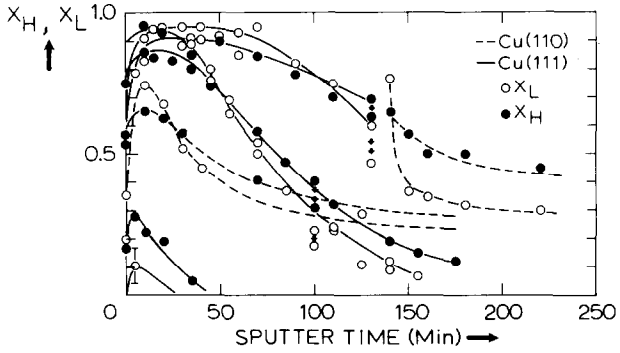

Fig. 5. Changes in x_H and x_L as a function of sputter time at room temperature: (— — —) Cu(110), (———) Cu(111). Arrows show the effect of a 16 h delay. Note that during this time the amount of Ni near the surface decreases.

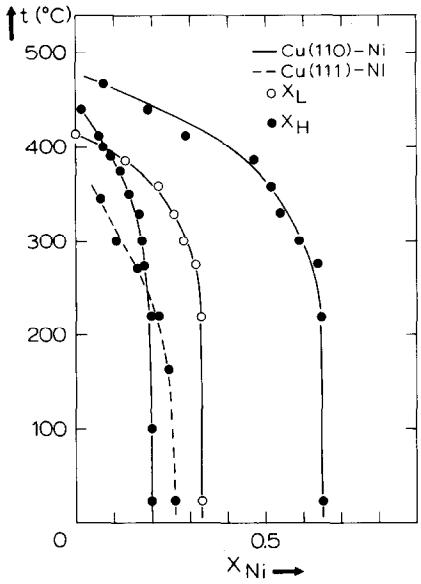

Fig. 6. Amount of Ni in the surface layers for Cu(110)–Ni and Cu(111)–Ni at different temperatures. With increasing temperature Ni is seen to dissolve completely in the Cu crystal.

crystal temperature for different amounts of nickel deposited on both Cu(111) and Cu(110).

4. Discussion

4.1. Room temperature experiments

At room temperature the adsorption of $Ni(CO)_4/CO$ gas mixtures at a Cu(110) surface saturates at a value of $\delta\psi = 0.3°$ and mol fraction of nickel in the first two and six layers of $x_L = 0.15$ and $x_H = 0.15$ respectively. For Cu(111) the corresponding values are $\delta\psi = 0.4°$ and $x_L = 0.26$ and $x_H = 0.22$. Since Auger spectra show both carbon and oxygen to be present, some sort of $Ni(CO)_x$ species must exist on the surface. This may be either partially decomposed nickel carbonyl or physisorbed $Ni(CO)_4$. Because of the following experimental evidence it is likely to assume that both species are present at the surface: (i) The decrease in $\delta\Delta$ after evacuating the system can be ascribed to CO desorption, as has been done in ref. [2] for a Cu(110)–Ni(1°) surface exposed to CO. Apparently no desorption of $Ni(CO)_4$ takes place since $\delta\psi$ remains constant. (ii) Adsorbed CO can be removed by heating the crystal before performing an AES measurement (which always leads to some disproportionation of CO). (iii) The amount of nickel, as revealed by the low energy Auger transitions, $x_L = 0.15$, is too large to be ascribed only to adsorbed nickel carbonyl molecules. The mean area of a nickel carbonyl molecule is 0.25 nm^2 [8] and the area of the Cu(110) unit cell is 0.093 nm^2, so it is obvious that nickel carbonyl remains at the surface. Strictly based on geometrical data, the maximum monolayer coverage of $Ni(CO)_4$ on Cu(110) is $\theta_{Ni(CO)_4} = 0.37$, on Cu(111) $\theta_{Ni(CO)_4} = 0.23$. Saturation then occurs when the whole surface is covered with one monolayer of $Ni(CO)_4$, since the actual pressure is much lower than the critical pressure at room temperature to form multilayers of nickel carbonyl. Performing the calculations as done by Webber et al. [5] to obtain the calculated amount of nickel, one finds $x_{L,calc} = 0.08$ (using a mean free escape depth of low energy Auger electrons of 3.7 Å, a nickel fraction in the first layer of 0.37 and zero in the second and following layers). This calculated fraction of nickel is significantly lower than the experimental value, so one can conclude that besides physisorbed nickel carbonyl also partially or completely decomposed $Ni(CO)_4$ has to be present at the surface.

Kishi et al. [8] measured with XPS that $Ni(CO)_4$ adsorbs, and partially decomposes, at an iron film at 90 K. After heating the film to 290 K they observed only atomic nickel to be present due to desorption and decomposition of nickel carbonyl. Palladium films at 90 K adsorb nickel carbonyl only molecularly, whereas at 290 K only atomic nickel is present at the surface. A remarkable difference is the amount of nickel which at room temperature can be deposited at the surfaces of both films with respect to the Cu(110) single crystal. On both metals the amount could increase to 100% of a mono-atomic nickel layer, as still no saturation occurred, whereas on Cu(110) at most an amount of $x_L = 0.15$ could be reached. This is probably due to the form in

which nickel is present at the surface and the structure of the surface itself. It has been shown that already at a rather low crystal temperature of 150°C, nickel atoms are able to penetrate the surface of a Cu(100) crystal [1] after being deposited via nickel carbonyl. In this paper we show that nickel, after being deposited at room temperature, disappears from the first surface layers when the crystal temperature was increased. It is also well known that diffusion or migration is much faster than in single crystals, due to the presence of grain boundaries. The differences in amounts of nickel which can be deposited on iron and palladium films and on a Cu(110) single crystal can then be explained by assuming that at films, even at room temperature, nickel atoms do not remain at the outermost surface layer but are able to penetrate to deeper layers.

4.2. Experiments at 220°C

The interaction of $Ni(CO)_4$ with Cu(110) and Cu(111) at a crystal temperature of 200°C is very similar that on Cu(100) above 150°C [1]. The changes in $\delta\Delta$, $\delta\psi$, x_L and x_H occur in the same way, although there is a slight difference in the values of $\delta\Delta$, $\delta\psi$ and x_H for which x_L is no longer zero (see table 1). The amount of nickel in the near surface layer (as measured by x_L) starts to increase for higher values of x_H in going to the more open copper surfaces. This suggests that the actual penetration of nickel into the crystal is easier for the more open surfaces. The same conclusion can be drawn from the data of penetrated nickel at constant $\delta\psi$, i.e. at a constant amount of nickel in the first few hundred layers, as measured by ellipsometry. For the densely packed Cu(111) face, the mole fraction of nickel in the first 6–8 layers (x_H) is significantly higher than for the more open faces (see table 1). Moreover, on Cu(111), removal of the $Ni(CO)_4$/CO gas pressure did not cause $\delta\psi$ to become constant immediately, as was the case for Cu(110). This also points to a slower penetration process from this more closely packed face.

From total exposures and estimated amounts of $Ni(CO)_4$ an upper limit of

Table 1
Comparison of Ni deposition on different Cu surfaces; the top two lines give the average Ni fraction in the first 6–8 layers and the corresponding $\delta\psi$ values when the Ni 101 eV first appears; the second two lines give the amount of Ni at constant $\delta\psi = 1$; for comparison the atomic density is given

	Cu(111)	Cu(100)	Cu(110)
x_H	0.15	0.10	0.25
$\delta\psi$ (deg)	0.5	0.7	1.1
$\delta\psi$ (deg)	1.0	1.0	1.0
x_H	0.45	0.30	0.20
Atomic density	$2.31/a^2$	$2.00/a^2$	$1.41/a^2$

the amount of nickel deposited on the crystals may be calculated. In all cases this is negligible, compared to the number of copper atoms in the crystals. This can also be deduced from the time needed to sputter-clean the surface alloy crystals. One would thus expect that eventually a homogeneous mixed crystal would be formed, with overall nickel content of about zero. Although at high nickel mol fractions some relaxation is observed (see fig. 4), this does not happen for lower initial amounts of nickel and, moreover, in all cases a (meta)stable surface alloy results. The initial decrease in x_H and x_L, after large amounts of nickel have been deposited, upon evacuation can be explained by a CO induced nickel segregation during deposition. It has been shown that even at room temperature CO is able to attract Ni to the surface [2]. After evacuation, the amount of Ni re-distributes to a steady state depth profile. This somewhat unusual non-uniform Ni distribution (see fig. 5) can in fact be metastable as shown in a separate publication [9]. Similar considerations apply to a sputtered surface. As shown in fig. 5, the nickel content in the outer layers changes when the ion bombardment is interrupted and the system is allowed to equilibrate at room temperature. This process is expected to be very slow compared to the equilibration at 220°C. So a 12 h waiting period will certainly not produce the equilibrium nickel distribution appropriate for this temperature.

4.3. Depth profiles

We now turn to the sputter profiles given in fig. 5. In contrast to the well annealed Cu–Ni alloys, where it is generally accepted that the surface is enriched in copper (see ref. [10]), the literature is not unequivocal with respect to the surface composition of the sputtered alloys. Although there is no doubt about the preferential sputtering of copper from clean surface alloys, the depth profile of the altered layer [11] and especially the surface composition of the altered layer is ambiguous. With ion scattering Swartzfager et al. [12] measured the surface composition to be equal to the bulk composition. The depth profile showed a remarkable copper deficiency in the second and the third layer which monotonically decayed towards the bulk composition. With AES [13–15] and SIMS [16] it was shown that the surface composition of the altered layer was enriched in nickel with respect to the bulk. A depth profile showed a monotonic decrease towards the bulk concentration. The instant increase in Ni content, observed in fig. 5, is much larger than any increase observed with AES due to sputtering of a Cu–Ni alloy at room temperature. From this we conclude that it is not just a matter of preferential sputtering of copper, but an actual higher Ni content in layers below the surface. Since x_L and x_H are essentially equal after 5 min of sputtering, which suggests the same average amount of nickel in about 3 and 8 layers, this nickel enrichment cannot be due to a depletion of copper in the following layers [12].

In order to obtain a more quantitative picture of the Ni depth profile we use the following equation [12], which pertains to an altered layer near the surface (mol fraction of nickel x^s) and a bulk-like layer behind it with mol fraction of nickel $x^b(z)$, depending on distance from the original surface:

$$\frac{dx^s}{dt} = -IS_{Ni}x^s + x^b(z)\, I\left[x^s S_{Ni} + (1-x^s)S_{Cu}\right] + P_{bs}x^b(z) - P_{sb}x^s, \tag{1}$$

where x^s is the average amount of Ni in the altered layer, x^b the fraction of Ni at depth z below the original surface, I the total ion flux (ions/s), S the sputter coefficient (atoms/ion), P_{bs} the probability of a Ni atom jumping from bulk to surface, and P_{sb} the reverse probability.

When the ion beam is switched off, x^s will change due to diffusion or segregation from or towards the surface. We did not observe an immediate change in both x_L and x_H when the ion beam was switched off. Only after 12 h the amounts had changed, as indicated in fig. 5. Therefore the last two terms of eq. (1) are small with respect to the sputtering time. Neglecting these terms, the solution of eq. (1) is given by the following equations, taking $x^s(0) = 0$ (see also ref. [14]):

$$x^s(t) = \frac{x^b(z)}{\left(1-x^b(z)\right)R + x^b(z)} \times \left\{1 - \exp\left\{-It\left[S_{Ni}\left(1-x^b(z)\right) + S_{Cu}x^b(z)\right]\right\}\right\}, \tag{2}$$

$$R = S_{Ni}/S_{Cu}. \tag{3}$$

In eq. (2) the first term gives the dependence of $x^s(t)$ on $x^b(z)$, when no more change in $x^s(t)$ occurs due to preferential sputtering. The exponential term in

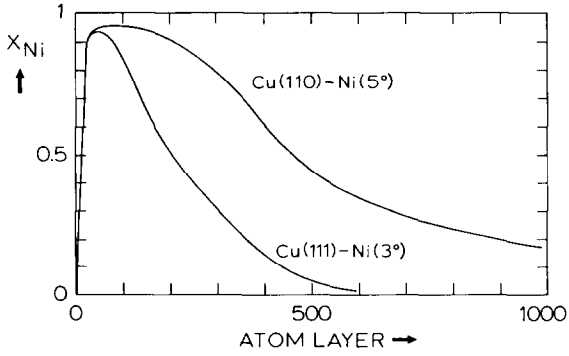

Fig. 7. Depth profile of Ni in Cu(111) and Cu(110), calculated from the data in fig. 5. The numbers in parentheses refer to the value of $\delta\psi$ at which the $Ni(CO)_4/CO$ exposure at 220°C was stopped. A higher value indicates a larger amount of nickel.

eq. (2) is much smaller than unity for times of the order of minutes (taking $I = 5 \times 10^{-6}$ A/cm^2, $S_{Ni} = 1.3$ and $S_{Cu} = 2$). Fig. 7 shows the depth profile for Ni, deposited from $Ni(CO)_4$, in Cu(111) and Cu(110). In converting the data to a distance scale, we have assumed that on the average 1.8 surface atom (either copper or nickel) is removed per incident Ar^+ ion.

4.4. Thermodynamic aspects

As remarked before, our surface alloys cannot be in true thermodynamic equilibrium, since the macroscopic composition is almost pure copper. A miscibility gap has been reported for the Cu–Ni system [17], which at 200°C leads to coexisting phases of composition 29% Ni and 98% Ni. Nevertheless our surface remained stable (apart from CO or O_2 induced segregation effects) for days at very different (sub)surface concentrations. Fig. 6 shows the composition–temperature diagram for our surface alloys. Equilibrium was reached after an increase in temperature in a period of some 10 to 20 min. It can be seen from this figure that the concentration of nickel rises in going into the crystal (x_L, the average amount of nickel in the first few layers is always less than x_H, the average amount in a larger number of layers). The difference between x_H and x_L becomes smaller at higher temperature, which implies a "flatter" Ni profile as a function of distance from the surface. Finally, around 400–450°C, complete dissolution of all nickel takes place as dictated by thermodynamics. One can thus assign a critical temperature of about 450°C to our surface alloys, below which a non-uniform concentration profile is metastable. This value may be compared with the wide range of 100–800°C [18] reported for bulk alloys.

4.5. Ellipsometric calculations

In order to rationalize the ellipsometric results accompanying nickel deposition and penetration (fig. 2), we have used the standard model of an overlayer (Cu–Ni) on a pure substrate (Cu). The dielectric constant of the overlayer (ϵ) was taken to be given by the Lorentz–Lorenz expression [19]

$$\frac{\epsilon - 1}{\epsilon + 2} = f_{Cu}\frac{\epsilon_{Cu} - 1}{\epsilon_{Cu} + 2} + f_{Ni}\frac{\epsilon_{Ni} - 1}{\epsilon_{Ni} + 2}, \tag{4}$$

where the f_i denote mol fractions.

If the substrate and adsorbed layer are considered isotropic, and $f_{Cu} + f_{Ni}$ is taken equal to one, it is not possible to calculate values of Δ and ψ, for any thickness of the adsorbed layer between 1–1000 Å, which are even in qualitative agreement with the observed changes in Δ and ψ. Guided by experience from ellipsometric measurements on silicon, where in some systems a fraction of voids is necessary to obtain agreement with measured optical constant over

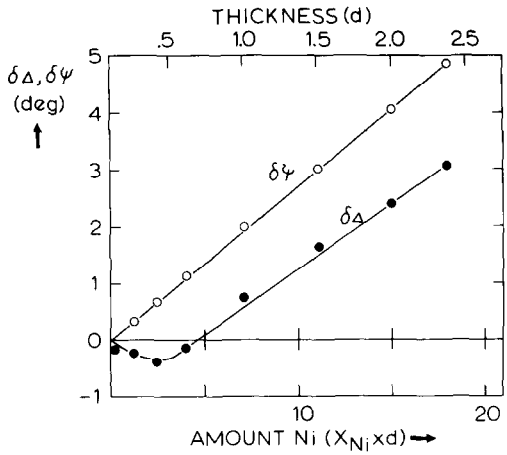

Fig. 8. Theoretical $\delta\Delta$ and $\delta\psi$ for a Cu/Ni overlayer with vacancies on a pure copper substrate. The total amount of Ni (mol fraction times layer thickness) is given on the lower axis, the corresponding layer thickness (in nm) on the upper axis. Due to the assumed step function for the concentration profile, these thicknesses differ from those in fig. 7.

a large spectral region [20], we have also used a variable fraction of "vacuum" in eq. (4). This amounts to putting $f_{Cu} + f_{Ni} < 1$, since $\epsilon_{vacuum} = 1$. In this case we are able to calculate values for Δ and ψ which are even quantitatively in agreement with the data in fig. 2 (see fig. 8). The fraction of voids must then be 1/10 of the fraction of nickel in the overlayer. From this assumed overlayer one may in turn compute values for the mol fractions x_H and x_L as measured by AES, taking into account the electron escape depth. These are also in good agreement with experiment. It thus seems that voids do occur in our surface alloys and they might account for the observed change of x_L and x_H with time (fig. 4) or temperature (fig. 5). Since they facilitate diffusion processes, but only in the region where the voids occur, they affect the Cu–Ni layer mainly near the surface and will inhibit complete dissolution of all nickel atoms.

5. Conclusions

(1) Adsorption of $Ni(CO)_4$ on copper surfaces at room temperature leads to adsorbed $Ni(CO)_x$ species with $x = 0, 1, \ldots, 4$.

(2) Adsorption of $Ni(CO)_4$ at 220°C leads to complete dissociation of the nickel carbonyl, no CO, C or O remaining on the surface. Nickel is deposited initially in deeper layers of the crystal, but close enough to the surface to be measurable with AES. Penetration of nickel is easier on the more open crystal faces.

(3) Sputter profiles show that the Ni content of the crystal increases in going into the crystal and may reach values close to unity before decaying again to zero over about 500–2000 layers.

(4) A critical temperature of 400–450°C may be assigned to the surface alloys, below which this non-uniform Ni distribution is (meta)stable.

(5) Ellipsometry indicates that in the Cu–Ni layer a significant fraction of voids are present which facilitate inter-diffusion and chemisorption induced segregation.

Ackowledgements

The authors thank Mr. A.J.M. Mens for technical assistance. The investigations were supported by the Netherlands Foundation of Chemical Research (SON) with financial aid from the Netherlands Organization for the Advancement of Pure Research (ZWO).

References

[1] C.A. Pietersen, C.M.A.M. Mesters, F.H.P.M. Habraken, O.L.J. Gijzeman, J.W. Geus and G.A. Bootsma, Surface Sci. 107 (1981) 353.
[2] C.M.A.M. Mesters, A.F.H. Wielers, O.L.J. Gijzeman, J.W. Geus and G.A. Bootsma, Surface Sci. 115 (1982) 237.
[3] C.M.A.M. Mesters, A.F.H. Wielers, O.L.J. Gijzeman, G.A. Bootsma and J.W. Geus, Surface Sci. 117 (1982) 605.
[4] F.C. Schouten, E.W. Kaleveld and G.A. Bootsma, Surface Sci. 63 (1977) 460.
[5] P.R. Webber, L.E. Rojas, P.F. Dobson and D. Chadwick, Surface Sci. 105 (1980) 20, and references therein.
[6] H. Albers, J.M.M. Broog and G.A. Bootsma, Surface Sci. 64 (1977) 1.
[7] G.A. Bootsma and F. Meyer, Surface Sci. 14 (1969) 52.
[8] K. Kishi, Y. Motoyoshi and S. Ikeda, Surface Sci. 105 (1981) 313.
[9] O.L.J. Gijzeman and H.N.W. Lekkerkerker, Chem. Phys. Letters 95 (1983) 52.
[10] C.R. Hehns, J. Catalysis 36 (1975) 114.
[11] N. Saeki and R. Shimizu, Surface Sci. 71 (1978) 479.
[12] A.G. Swartzfager, S.B. Ziemecki and M.J. Kelley, J. Vacuum Sci. Technol. 19 (1981) 185.
[13] M.L. Tarring and G.K. Wehner, J. Appl. Phys. 42 (1971) 2449.
[15] R. Shimizu and N. Saeki, Surface Sci. 62 (1977) 751.
[16] F. Toyokawa, K. Furuya and T. Kikuchi, Surface Sci. 110 (1981) 329.
[17] W.M.H. Sachtler and P. van der Plank, Surface Sci. 18 (1969) 62.
[18] P.E.C. Franken and V. Ponec, J. Catalysis 42 (1976) 398, and references therein.
[19] L. Lorenz, Ann. Physik. Chem. 11 (1880) 70.
[20] D.E. Aspnes, Thin Solid Films 89 (1982) 249.